

Flexible Boundary Design for a Chattanooga Microgrid Powered by Landfill Solar Photovoltaic and Battery Storage

Samuel Okhuegbe¹, Chengwen Zhang¹, Dong Jiaojiao¹,
Yilu Liu^{1,2}
University of Tennessee¹, Oak Ridge National Laboratory²
Knoxville, USA.
{sokhuegb, czhang70}@vols.utk.edu, {jdong7, liu}@utk.edu

Austin Walker, Jim Glass
Electric Power Board of Chattanooga
Chattanooga, USA.
{walkeram, glassjb}@epb.net

Abstract— Landfill based microgrids powered by renewable energy aid reliability and resiliency while promoting environmental and energy justice. This paper aims to design a flexible boundary algorithm for a proposed Chattanooga landfill microgrid with the ability to shrink or expand its boundaries based on the available power from the solar PV and battery storage. This helps to improve resiliency unlike the conventional fixed boundary microgrids. The flexible boundary algorithm determines the combination and switching status of the intellirupter® which changes the microgrid boundaries to achieve power balance by dropping or energizing specific load sections. The microgrid with flexible boundary was simulated in MATLAB/Simulink and performed satisfactorily when tested under various scenarios.

Index Terms— Flexible Boundary, Intellirupter®, Landfill, Microgrid, Renewable Energy.

I. INTRODUCTION

Microgrids powered by distributed renewable energy play an important role in the transition towards a cleaner and sustainable energy grid [1]. Among various renewable energy sources, there is an increasing trend of integrating solar photovoltaic (PV) in distribution networks to form microgrids, due to the reduced cost of solar panels, improved efficiency of solar panels and advancements in inverter technology [2]. Energy storage such as batteries are needed to improve the overall reliability and resiliency of the microgrids by providing a voltage/frequency source and extending the operation of the microgrid when solar power is not available. Repurposing closed landfill sites to host solar PV/battery storage creates a sustainable opportunity to use lands with little reuse value while reducing land usage conflict with agricultural, recreational, and economic activities. Closed landfills are ideal locations for siting community solar PV as they are usually large tract of unused lands with good irradiation, little shading and close to the community [3]. Landfills are historically situated in disadvantaged and minority communities and as such repurposing these landfill sites for a solar PV/battery project would help create jobs and stimulate the local economy while

providing clean energy near the load center. This helps to improve environmental, social and energy justice [4].

Microgrids are traditionally designed with fixed electrical boundaries, and this puts a very conservative restriction on the sizing and operation of the microgrid as they are expected to serve the same amount of load despite the intermittent nature of the distributed renewable energy source [5], [6]. Flexible boundaries allow the microgrid to expand or shrink its boundaries to pick up or drop certain loads while trying to maintain power to the critical infrastructure. This capability allows the microgrid to maintain active and reactive power balance regardless of faults, power changes in the intermittent sources and loads. Various research has been conducted to design flexible boundaries for various microgrid networks. Researchers in [7] propose the use of clustering techniques to create dynamic microgrid boundaries. Researchers in [5] applied the shortest route algorithm and linear programming to determine the optimal intellirupters® to open or close to change the boundaries while achieving power balance. It also accommodates changes in network topology and multiple source location. Researchers in [8] used a tree-based approach to choose the best smart switches to open or close for each load section thereby shedding or restoring loads, while researchers in [9] developed a strategy to determine the on-off operation of smart switches for fault isolation and load restoration in a distribution network. Mixed integer linear programming was applied by researchers in [10] to maximize service to the critical load while remotely controlling the ON/OFF status of the switching devices and distributed generators.

This work offers a less complex and bespoke flexible boundary design for a Chattanooga distribution feeder with the network topology and source location already known and eliminates the need for optimization techniques. The aim of this work is to determine the optimal switching status and combination of the intellirupters to expand or shrink the microgrid boundary to maintain active and reactive power balance between the supply and load. The Chattanooga microgrid is powered by a landfill solar PV and battery. The flexible boundary algorithm also accommodates fault isolation

This work was supported by the Electric Power Board (EPB) of Chattanooga and the Center for Ultra-Wide-Area Resilient Electric Energy Transmission Network (CURENT)

and operates only when the microgrid is islanded from the grid. Such a scenario might occur when there is a contingency on the main grid which would require the microgrid to maintain resiliency by supplying power to the critical and non-critical loads based on power availability, with priority given to the critical loads. In grid connected mode, there is no need for a flexible boundary, as the grid power is sufficient to pick up any load not met by the Solar PV/Battery.

II. CASE STUDY MICROGRID DESCRIPTION AND SIMULATION SETUP

The proposed landfill based microgrid takes advantage of an existing distribution feeder infrastructure located in Chattanooga, Tennessee. The microgrid feeder topology is shown in Fig.1 and makes use of intelligent switching devices known as intellirupters [11]. The intellirupters are labeled SW1 to SW12, with the circuit breaker labeled BRK. The microgrid has multiple points of connection to the grid through other connected feeders. For designing and simulating the flexible boundary, the microgrid would only be evaluated in stand-alone mode, and as such SW8, SW9, SW10, SW11, SW13, SW14 and BRK would always be opened. The solar photovoltaic and battery are placed at the landfill location and stepped-up to the feeder line voltage (VLL) which is 12.47 kV. The radial feeder topology is separated into load sections from load section 1 (L_1) through to load section 8 (L_8) based on the intellirupter location.

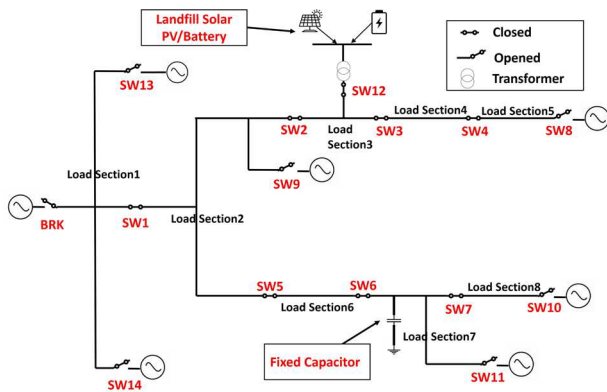


Fig.1 Chattanooga landfill microgrid topology

The simulation was set up using MATLAB/Simulink, with the solar PV inverter in grid-following and the battery inverter in grid-forming mode based on the modified work done in [12]. A 3 MW solar PV and 3 MWh battery Storage is used in this work. A fixed capacitor is located at load section7 which supplies reactive power if that load section is picked. The net reactive power demand at load section 7 can be easily modified based on the reactive power of the fixed capacitor. Under normal conditions, the load is supplied by the solar PV operating under maximum power point tracking. The battery charges when excess power from the solar PV is available and discharges when the power from the solar PV is insufficient to meet the load. The battery inverter also supplies or absorbs the needed

reactive power by the load. In this case study, load section 3 is taken as the critical load as it is the community closest to the landfill site. It is assumed that the disadvantaged communities are located close to the landfill site.

III. FLEXIBLE BOUNDARY DESIGN FOR CHATTANOOGA MICROGRID

Given the power available from the landfill solar PV/battery, the flexible boundary algorithm determines which load section combination to pick up or drop to maintain active and reactive power balance between supply and load. The algorithm selects the load section combinations that feed the maximum total load without exceeding the available supply; these load sections become the optimal load section combination. The algorithm then determines which intellirupter to open or close based on the selected optimal load section combination.

A. Critical Load and Feasible Load Section Combinations

To design an efficient flexible boundary algorithm for the Chattanooga microgrid, knowledge of the critical load and feasible load combination is required. In this topology the critical load is coincidentally load section 3 (L_3) and no load section can be energized without energizing load section 3. That means all feasible load section combinations must include load section 3. This inherently means there is no need for any extra design to accommodate load section 3. However, if the critical load was in any other load section, then all load sections along the path leading to the critical load section must be energized first before other non-critical load sections can be energized. For example, if load section 5 was the critical load, then load section 3, 4 and 5 must always be energized and any excess power can then be used to pick up the other load sections.

The load sections must be combined in a specific way based on the feeder topology, for example a combination of load section 6, 7, 8 is not feasible because power has to flow through load section 3 and load section 2 before it flows to load section 6,7,8. Since the microgrid feeder topology is known there is a limited number of feasible load sections which can be easily itemized.

B. Relationship Between Topology, Load Section and Intellirupter Combination

The microgrid total load P_{load} can be expressed in terms of the switching status of the intellirupter as shown in (1).

$$P_{load} = L_1(SW1 * SW2 * SW12) + L_2(SW2 * SW12) + L_3(SW12) + L_4(SW3 * SW12) + L_5(SW3 * SW4 * SW12) + L_6(SW2 * SW5 * SW12) + L_7(SW2 * SW5 * SW6 * SW12) + L_8(SW2 * SW5 * SW6 * SW7 * SW12) \quad (1)$$

Where L_1 to L_8 are load sections 1 through to load section 8, and SW1 to SW12 are the intellirupters with values of either 1 or 0 which represent ON or OFF state. For instance, for power to get to load section 1 (L_1), intellirupter SW1, SW2 and SW12 must be ON, the same logic goes for the other load sections.

$$A = \begin{bmatrix} -1 & 1 & 0 & 0 & 0 & 0 & 0 & 0 & 0 & 0 & 0 & 0 & -1 & -1 \\ 0 & -1 & 1 & 0 & 0 & -1 & 0 & 0 & 0 & -1 & 0 & 0 & 0 & 0 \\ 0 & 0 & -1 & -1 & 0 & 0 & 0 & 0 & 0 & 0 & 0 & 0 & 1 & 0 \\ 0 & 0 & 0 & 1 & -1 & 0 & 0 & 0 & 0 & 0 & 0 & 0 & 0 & 0 \\ 0 & 0 & 0 & 0 & 1 & -1 & 0 & 0 & 0 & 0 & 0 & 0 & 0 & 0 \\ 0 & 0 & 0 & 0 & 0 & 1 & -1 & 0 & 0 & 0 & 0 & 0 & 0 & 0 \\ 0 & 0 & 0 & 0 & 0 & 0 & 1 & -1 & 0 & 0 & 0 & -1 & 0 & 0 \\ 0 & 0 & 0 & 0 & 0 & 0 & 0 & 1 & 0 & 0 & -1 & 0 & 0 & 0 \end{bmatrix} \quad (2)$$

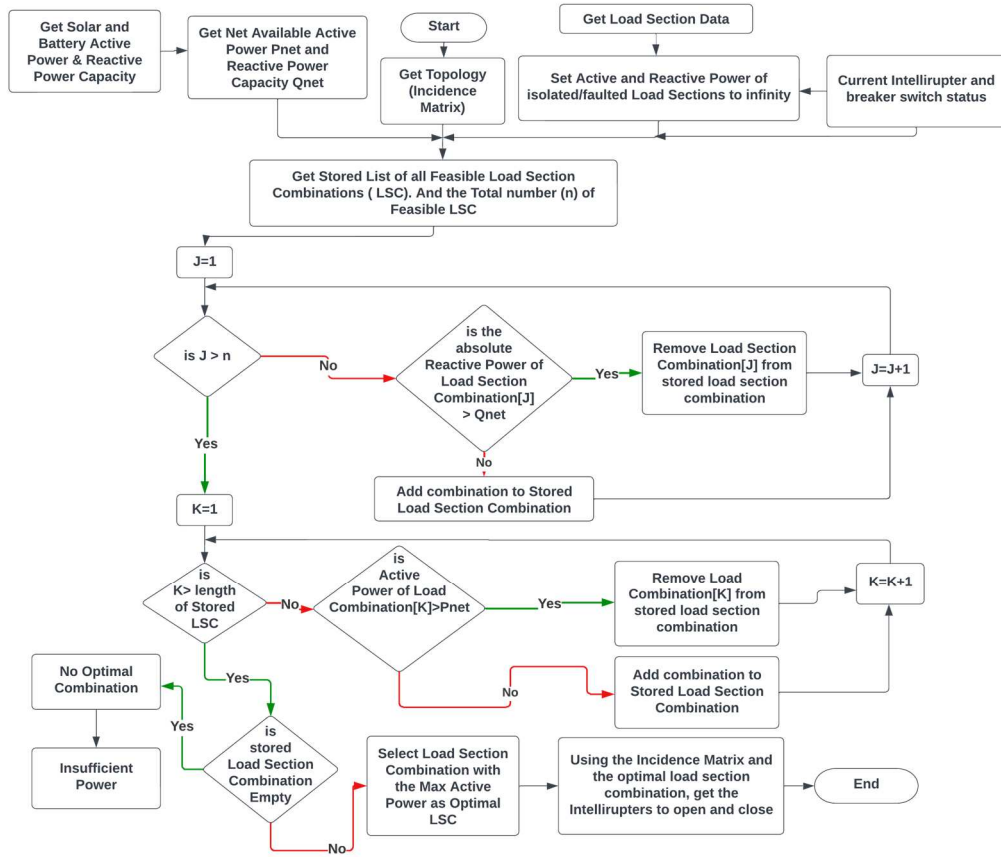


Fig. 2 Flexible boundary algorithm for Chattanooga landfill based microgrid.

The flexible boundary algorithm uses this information to know which intellirrupter must be closed to pick up a particular load section.

The topology of the Chattanooga microgrid is an important input to the flexible boundary algorithm. The incident matrix can be used to represent the topology of the microgrid feeder, using the intellirrupters and breaker as nodes (columns) while the load sections as elements (rows). It shows all the switching devices associated with each load section. The direction of the incident matrix is not relevant for this work and as such the direction can be taken arbitrarily. Though in this work we assume power flows from the SW12 node where the source is located into the other intellirrupter nodes. The direction determines the positive or negative signs in the incidence

matrix. The incidence matrix for the Chattanooga microgrid can be seen in (2). The columns are the nodes, which start from BRK then SW1 sequentially through to SW14. Column 1 is BRK, column 2 through to column 15 is SW1 to SW14. The rows are the load sections from load section 1 sequentially through to load section 8, with row 1 being load section 1.

The information obtained from (1) and (2) can then be easily used to determine which intellirrupter to open or close based on an optimal load section combination. For example, based on the available power, if the optimal load section combination is L_2 and L_3 , then from (1) we know we need to close SW2 and SW12. From (2) the associated devices are SW1, SW2, SW3, SW5, SW9 and SW12, where L_2 (row 2) is connected to SW1, SW2, SW5 and SW9 (column 2,3,6 and 10) and L_3 (row 3) is connected to SW2, SW3 and SW12 (column 3,4 and 13). The difference between the devices to close (SW2-SW12)

determined from (1) and the associated devices (SW1-SW2-SW3-SW5-SW9-SW12) obtained from (2) would give you the minimum devices to open which in this example is SW1, SW3, SW5 and SW9.

C. Isolated and Faulted Section

The flexible boundary algorithm handles isolated sections using the principle that opened circuits have theoretically infinite impedance. Therefore, the algorithm assumes that the load sections associated with any isolated/opened intellirupter would have an infinitely high load demand. As a result, those load sections would never be picked up or energized. For example, if SW3 is opened due to a fault, then load section 4 and 5 would be assumed to have an infinite load demand. This would ensure that regardless of the supply available from the solar PV/battery, SW3 would not be closed and load section 4 and 5 would never be energized.

D. Flexible Boundary Algorithm and Principle of Operation

The flexible boundary algorithm determines the intellirupter combination to open or close to shrink or expand the microgrid boundaries to achieve active and reactive power balance between supply and load. The algorithm determines the optimal boundary that would supply the maximum amount of active power load while ensuring the reactive power limits are not exceeded. Fig. 2 shows the flow chart of how the flexible boundary algorithm operates. The algorithm reads the inputs which includes the active and reactive power of the solar PV/battery, active and reactive demand of each load section, feeder topology and initial switching status of the intellirupter. Next all feasible load section combinations are obtained. A reactive power screening of each feasible load section combination is done. Feasible load section combinations that are less than or equal to the net available reactive power supply are stored. Then an active power screening is done to these stored feasible load section combinations. Feasible load section combinations where the active power demand is less than or equal to the available active power from the supply are stored. Basically, we have screened off feasible load section combinations that violate either the active or reactive power limit, and we would be left with only feasible load section combinations that are within active and reactive power currently available from the supply. The feasible load section combination with the maximum active power demand is then selected as optimal load section combination. This way the microgrid feeds as much load as possible while achieving power balance. The algorithm then determines the intellirupter switching status based on this optimal load section combination.

IV RESULTS AND DISCUSSION

A. Flexible Boundary Under Normal Conditions

The flexible boundary algorithm was simulated under normal conditions without any isolated sections for 10 seconds. Fig. 3 shows the power exchange between the supply and load. As the boundaries change the voltage in the microgrid is maintained at 12.47 kV, this can be observed in Fig 6. Fig. 4 and Fig 5 shows the switching status of the breaker and intellirupter as certain load sections are picked up or dropped. From Fig 5, all the switching devices at the point of connection

to the grid (BRK, SW8, SW9, SW10, SW11, SW13 and SW14) are all opened, and the flexible boundary algorithm never closes them, this ensures the system is islanded and the power exchanged at the point of connection (P_{pcc}) to the grid is zero as evident in Fig.3.

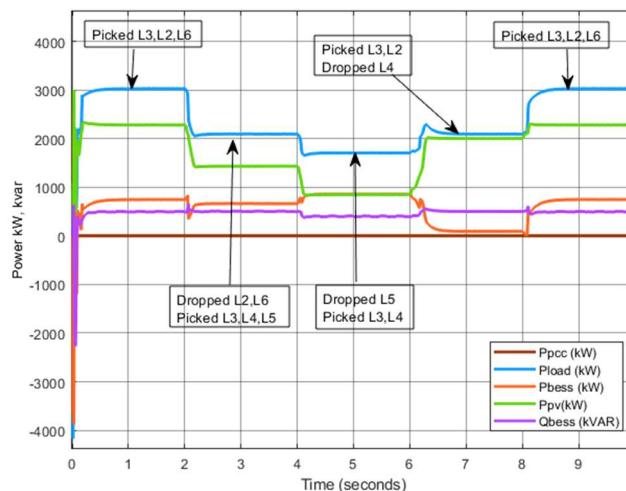


Fig. 3 Power flow between supply and load as the boundary change

From 0-2 seconds the solar PV and battery energizes load section L_3 , L_2 and L_6 by closing intellirupter SW12-SW2-SW5 while opening SW3-SW1-SW6. At 2 seconds, the power from the solar PV (P_{pv}) starts to ramp down and the flexible boundary algorithm reduces the total load served by dropping L_2 and L_6 while picking up L_4 and L_5 in addition to L_3 . To achieve this SW2 is opened while SW12-SW3-SW4 are closed as can be seen in Fig 4. Between 4-6 seconds the solar power further drops and the algorithm accommodates this by dropping more load sections. The battery discharges power (P_{bess}) within its capacity. At this stage load section L_5 is dropped leaving only L_3 and L_4 energized. This corresponds to closing SW12-SW3 and opening SW4-SW2. At 6-8 seconds the solar power increases and more load is served. Here load section L_3 and L_2 are energized with SW3-SW1-SW5 opened and SW12-SW2 closed. Lastly at 8-10 seconds the solar power further increases, and the algorithm picks up more load sections, with the battery discharging. At this point L_6 is picked up in addition to L_3 and L_2 , with SW12-SW2-SW5 closed and SW3-SW1-SW6 opened. The flexible boundary algorithm opens or closes the minimum number of switching devices needed to achieve a certain balance between the load and supply. The status of other switching devices remain as they were in previous time steps unless a change in switching status is required, this ensures we switch only the required devices. Fig 6 shows that the line voltage (VLL) in the microgrid is maintained at 12.47 kV, though very brief spikes are observed at time steps when the intellirupter switching takes place but then the voltage quickly returns to normal. All through the simulation the battery inverter supplied reactive power (Q_{bess}) as demanded.

B. Flexible Boundary Under Isolated Conditions

The exact same simulation was carried out but with SW4 deliberately opened to isolate load section 5 (L_5), which is a faulted section.

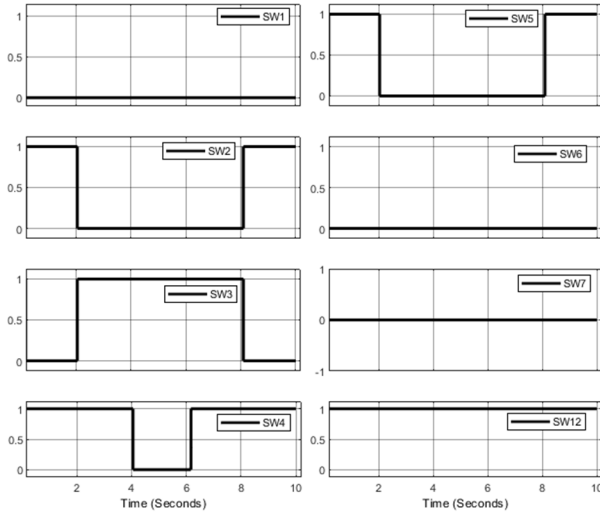


Fig. 4 Switching status of interrupters

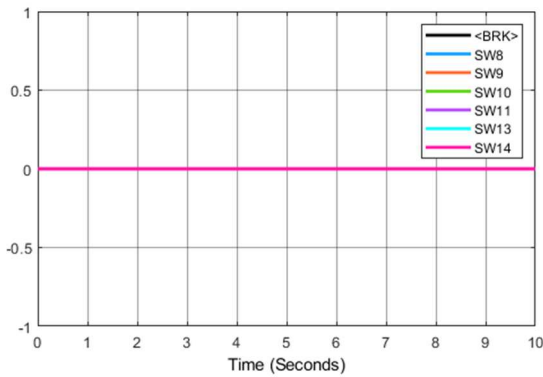


Fig. 5 Switching status of breaker and interrupter at point of connection to the grid.

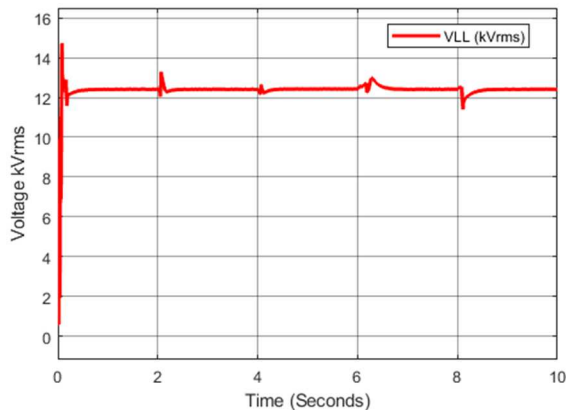


Fig. 6 Microgrid voltage during Interrupter Switching

From the switching status shown in Fig 8, we can observe that SW4 remained open and load section 5 was never energized. This is unlike the previous results where L_5 was energized at 2-4 seconds. Fig 7 shows the changes in the total load sections energized as the supply changes. From 0-2 seconds, L_3 , L_2 and L_6 are energized. This is the same as when there was no isolated section.

At 2 seconds the solar power starts to drop. Ideally load section 3,4 and 5 should be energized as was observed in the previous results, but because load section 5 is isolated, the flexible

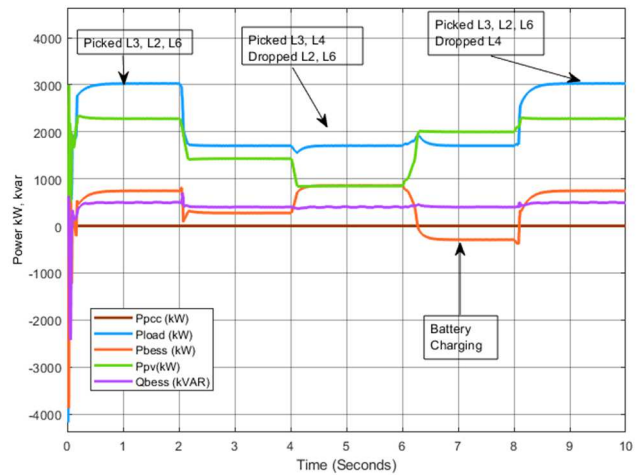


Fig 7 Power flow between supply and load as the boundary changes with an isolated load section.

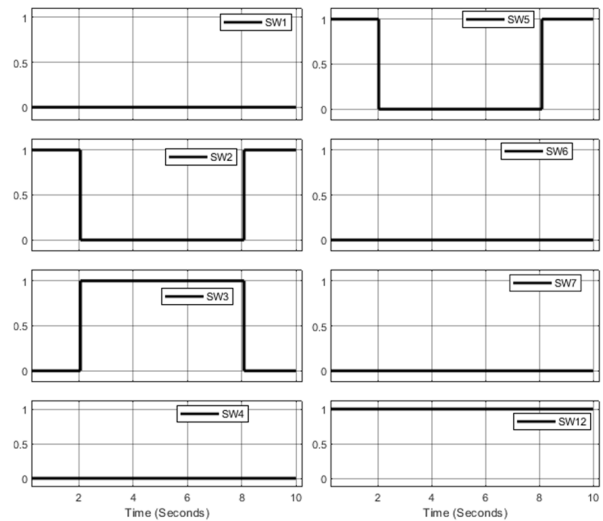


Fig 8 Switching status of interrupters with load section 5 isolated.

boundary algorithm energizes just L_3 and L_4 . This corresponds to closing SW12-SW3 and opening SW2. At 4-6 seconds the solar power drops further but the battery is sufficient to meet make up for this, and as such L_3 , L_4 remain energized and no change in the switching status. At 6-8 seconds the solar power increases but not enough to pick up extra load. So L_3 and L_4

still remain as the only connected load section. The extra power available from the solar PV is used to charge the battery.

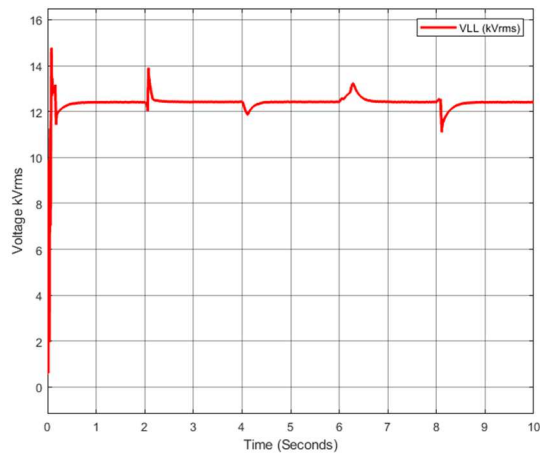


Fig 9. Microgrid voltage during intellirupter with an isolated section

At 8-10 seconds, the solar power further increases and the battery discharges to pick up more load. At this stage L_3 , L_2 and L_6 is energized with SW12-SW2-SW5 closed and SW3-SW1-SW6 opened. SW4 remains open all through. The voltage profile in Fig 9. shows brief voltage spikes that quickly settle at points when the intellirupters are switched on/off and at points when the solar power changes significantly causing the battery to react by supplying or absorbing power.

V. CONCLUSION

In this work a flexible boundary algorithm was designed for a proposed Chattanooga microgrid powered by landfill solar PV and battery. The algorithm determines the best intellirupter combination to open or close to pick up or drop load sections to achieve active and reactive power balance. The algorithm tries to pick up the maximum load possible without exceeding the available power from the solar PV and battery. The system was simulated in MATLAB/Simulink with and without a faulted isolated section and performed successfully.

REFERENCES

- [1] M. Debouza, A. Al-Durra, T. H. M. EL-Fouly, and H. H. Zeineldin, "Survey on microgrids with flexible boundaries: Strategies, applications, and future trends," *Electric Power Systems Research*, vol. 205, Apr. 2022, doi: 10.1016/j.epsr.2021.107765.
- [2] R. Panigrahi, S. K. Mishra, S. C. Srivastava, A. K. Srivastava, and N. N. Schulz, "Grid Integration of Small-Scale Photovoltaic Systems in Secondary Distribution Network - A Review," *IEEE Trans Ind Appl*, vol. 56, no. 3, pp. 3178–3195, May 2020, doi: 10.1109/TIA.2020.2979789.
- [3] M. Popkin and A. Krishnan, "The Future of Landfills Is Bright," *Rocky Mountain Institute*, pp. 2–28, 2021.
- [4] R. Ciriminna, L. Albanese, M. Pecoraino, F. Meneguzzo, and M. Pagliaro, "Solar Landfills: Economic, Environmental, and Social Benefits," *Energy Technology*, vol. 6, no. 4, pp. 597–604, Apr. 2018, doi: 10.1002/ente.201700620.
- [5] C. Zhang et al., "Real-Time Power Management for Microgrids With Dynamic Boundaries and Multiple Source Locations," *IEEE Access*, vol. 10, pp. 84120–84134, 2022, doi: 10.1109/ACCESS.2022.3197601.
- [6] S. Zhen, Y. Ma, F. Wang, and L. M. Tolbert, "Operation of a Flexible Dynamic Boundary Microgrid with Multiple Islands," in *2019 IEEE Applied Power Electronics Conference and Exposition (APEC)*, 2019, pp. 548–554.
- [7] A. Bernstein et al., "DynaGrid: Dynamic Microgrids for Large-Scale DER Integration and Electrification," 2022. Accessed: Apr. 07, 2023. [Online]. Available: <https://www.osti.gov/biblio/1891199>
- [8] X. Hu et al., "Real-time power management technique for microgrid with flexible boundaries," *IET Generation, Transmission and Distribution*, vol. 14, no. 16, pp. 3161–3170, Aug. 2020, doi: 10.1049/iet-gtd.2019.1576.
- [9] Y. J. Kim, J. Wang, and X. Lu, "A Framework for Load Service Restoration Using Dynamic Change in Boundaries of Advanced Microgrids with Synchronous-Machine DGs," *IEEE Trans Smart Grid*, vol. 9, no. 4, pp. 3676–3690, Jul. 2018, doi: 10.1109/TSG.2016.2638854.
- [10] C. Chen, J. Wang, F. Qiu, and D. Zhao, "Resilient Distribution System by Microgrids Formation after Natural Disasters," *IEEE Trans Smart Grid*, vol. 7, no. 2, pp. 958–966, Mar. 2016, doi: 10.1109/TSG.2015.2429653.
- [11] M. Ahmed, A. Ali, S. Mohammed, and K. Abdelrahman, "Investigation of Ferroresonance Incidents in the EPB Distribution Network," in *2018 IEEE Power & Energy Society General Meeting (PESGM)*, 2018.
- [12] Pierre Giroux, "Microgrid Dynamic Operation." 2023. Accessed: Apr. 08, 2023. [Online]. Available: https://www.mathworks.com/matlabcentral/fileexchange/93235-microgrid-dynamic-operation?s_tid=srchtitle